Conserved Cysteine 126 in Triosephosphate Isomerase Is Required Not for Enzymatic Activity but for Proper Folding and Stability†

Edith González-Mondragón,‡ Rafael A. Zubillaga,*,‡ Emma Saavedra,§,|| María Elena Chánez-Cárdenas,§,⊥ Ruy Pérez-Montfort,§ and Andrés Hernández-Arana*,‡

Área de Biofisicoquímica, Departamento de Química, Universidad Autónoma Metropolitana-Iztapalapa, Apartado Postal 55-534, Iztapalapa D.F. 09340, Mexico, and Departamento de Bioquímica, Instituto de Fisiología Celular, Universidad Nacional Autónoma de México, 04510 México D.F., Mexico

Received November 20, 2003; Revised Manuscript Received January 21, 2004

ABSTRACT: In triosephosphate isomerase, Cys126 is a conserved residue located close to the catalytic glutamate, Glu165. Although it has been mentioned that Cys126 and other nearby residues are required to maintain the active site geometry optimal for catalysis, no evidence supporting this idea has been reported to date. In this work, we studied the catalytic and stability properties of mutants C126A and C126S of *Saccharomyces cerevisiae* TIM (wtTIM). None of these amino acid replacements induced significant changes in the folding of wtTIM, as indicated by spectroscopic studies. C126S and C126A have K_M and k_{cat} values that are concomitantly reduced by only 4-fold and 1.5-fold, respectively, compared to those of wtTIM; in either case, however, the catalytic efficiency (k_{cat}/K_M) of the enzyme is barely affected. The affinity of mutated TIMs for the competitive inhibitor 2-phosphoglycolate augmented also slightly. In contrast, greater susceptibility to thermal denaturation resulted from mutation of Cys126, especially when it was changed to Ser. By using values of the rate constants for unfolding and refolding, we estimated that, at 25 °C, C126A and C126S are less stable than wtTIM by about 5.0 and 9.0 kcal mol^{-1}, respectively. Moreover, either of these mutations slows down the folding rate by a factor of 10 and decreases the recovery of the active enzyme after thermal unfolding. Thus, Cys126 is required for proper stability and efficient folding of TIM rather than for enzymatic catalysis.

Among the enzymes that are recognized as nearly perfect catalysts, triosephosphate isomerase (TIM,[1] EC 5.3.1.1) is one of the most studied. Through the use of diverse physical and molecular biology methods, it has been disclosed that this dimeric enzyme, which catalyzes the interconversion between dihydroxyacetone phosphate (DHAP) and D-glyceraldehyde 3-phosphate (DGAP), recruits several amino acid side chains to achieve its high catalytic efficiency. Three of these residues (Glu165, His95, and Lys12) are directly involved in catalysis and are regarded as essential for TIM activity; single mutation of each one of them (i.e., E165D, H95Q, or K12R) leads to drops in catalytic efficiency, k_{cat}/K_M, from 140- to 4000-fold (*1*−*3*). Not surprisingly, the three catalytic residues have been strictly conserved through evolution, as judged from an alignment made with more than 108 TIM sequences (encompassing organisms from Archaea to man) obtained from the Swiss-Prot database.

In addition to the essential catalytic residues, natural TIM variants display a large number of fully or highly conserved residues, most of them located in the C-terminal half of each monomer, which comprises the last four β-strand−loop−α repeats of its $(\beta/\alpha)_8$ barrel fold. Crystallographic studies with substrate analogues bound to the enzyme and with the unliganded enzyme, together with mutational studies, have helped us to understand the high conservation of many of these residues. For example, residues 170−173 (*Saccharomyces cerevisiae* TIM numbering) from loop 6 comprise the central part of the lid that closes upon substrate binding, forming a tight binding pocket (*4*, *5*); indeed, the amide nitrogen of Gly171 is hydrogen-bonded to one of the phosphate oxygens of substrate analogues (*4*, *6*). Examination of the binding pocket has revealed that additional hydrogen bonds are established between phosphate oxygens and the amide nitrogens of glycines 210, 232, and 233 and of Ser211 (*4*, *5*). Further direct ligand−enzyme contacts are restricted to those formed by the catalytic residues and Asn10 (*4*, *5*).

There is, however, a group of highly conserved residues that, though not in direct contact with the ligand, lie close to the catalytic side chains. Included in this group are Ser96, Glu97, Cys126, and Thr75 from the adjacent subunit, which

† This work was supported in part by CONACyT, México (41348-F, 32417-E), and DGAPA-UNAM (IN214202). E.G.-M. was supported by a fellowship from CONACyT (No. 130442).

* Address correspondence to either of these authors. A.H.-A.: fax, +52 (55) 5804-4666; e-mail, aha@xanum.uam.mx. R.A.Z.: fax, +52 (55) 5804-4666; e-mail, zlra@xanum.uam.mx.

‡ Universidad Autónoma Metropolitana-Iztapalapa.

§ Universidad Nacional Autónoma de México.

|| Current address: Departamento de Bioquímica, Instituto Nacional de Cardiología, México D. F. 14080, Mexico.

⊥ Current address: Departamento de Neuroquímica, Instituto Nacional de Neurología, y Neurocirugía, México D.F. 14269, Mexico.

[1] Abbreviations: TIM, triosephosphate isomerase; DHAP, dihydroxyacetone phosphate; DGAP, D-glyceraldehyde 3-phosphate; wtTIM, TIM from *Saccharomyces cerevisiae*; C126S and C126A, the *S. cerevisiae* TIM in which Cys126 has been replaced by Ser or Ala, respectively; TEA, triethanolamine; PCR, polymerase chain reaction; α-GDH, α-glycerophosphate dehydrogenase; PGA, 2-phosphoglycolate; ITC, isothermal titration calorimetry; CD, circular dichroism.

10.1021/bi036077s CCC: $27.50
Published on Web 02/21/2004

are also regarded as constituents of the active site (*4*, *7*). It has been proposed that Ser96 is involved in positioning the catalytic base Glu165 and two bound water molecules for optimal catalysis (*8*). No well-defined function has been ascribed to Glu97; as noted by Lolis et al. (*7*), however, the engagement of this side chain in a network of hydrogen bonds involving Lys12, and also Thr75 of the adjacent subunit, gives a hint on the role played by both Glu97 and Thr75. In this view, loop 3 (in which Thr75 is located) would provide part of the structural support for the active site of the other subunit, explaining why only the dimer of TIM is catalytically competent (*7*). Nevertheless, the point mutations E97D and S96T are reported to have no significant effect on the catalytic efficiency of chicken TIM (*9*), results that contrast with the notion that residues at positions 96 or 97 are conserved because of their role in maintaining a precise structure of the active site (*7*).

Likewise, not much is known about the possible catalytic function of Cys126, a residue located near the end of strand 5; its S_γ atom forms part of the β-barrel inner core, but it is also in van der Waals contact with one oxygen of the catalytic Glu (*5*). We noted previously that oxidation of Cys126 and Cys41 (the only two cysteines in *S. cerevisiae* TIM) with chloramine-T reduced the catalytic activity in about 50% (*10*). Harbury and collaborators (*11*) have recently reported that substituting Cys126 for Ala causes a significant destabilization of yeast TIM, as deduced from the enzyme unfolding induced by guanidinium chloride; however, the effect of the C126A mutation on enzymatic activity was not reported. The same group had previously found an apparent 13-fold drop of k_{cat}/K_M for the mutant C126V (*12*). Because in this case catalytic activity was determined directly from crude cellular extracts (of TIM-deficient *Escherichia coli*), the activity decrease could result from a reduction in the stability or the folding ability of the mutant (as the authors assumed) but also from alterations in the active site geometry.

It is clear that further investigations on the properties of TIM single mutants would greatly benefit our understanding of the reasons Cys126 and other active site residues are almost ever present in natural TIM variants. The present study focused on the effects of mutating Cys126; we constructed and expressed two single-point mutants of *S. cerevisiae* TIM in which Cys126 was changed to Ser or Ala, two of the most frequently observed substitutions of Cys in nature. Studies of their catalysis and rates for unfolding and refolding were carried out and compared with the properties displayed by the wild-type isomerase. Our results point out that mutation of Cys126 has no significant effect on the catalytic efficiency of TIM, but it is detrimental for the stability and folding speed of the protein.

MATERIALS AND METHODS

Mutagenesis, Protein Expression, and Purification. Substitution of the Cys residue at position 126 in *S. cerevisiae* TIM (wtTIM) for Ser or Ala was performed by overlap extension mutagenesis (*13*) with the polymerase chain reaction (PCR). The mutagenic oligonucleotides were as follows: 5′-GTCATCTTGTCCATCGGT-3′ (C126S forward) and 5′-ACCGATGGACAAGATGAC-3′ (C126S reverse); 5′-GTCATCTTGGCGATCGGT-3′ (C126A forward) and 5′-ACCGATCGCCAAGATGAC-3′ (C126A reverse). In both cases, the T7 promoter and T7 terminator oligonucleotides were used as flanking primers to amplify the complete gene. The mutated genes were cloned in the pET3a vector (pET System, Novagen); codon substitutions were confirmed by sequencing the complete genes. The resulting plasmids were used to transform BL21(DE3)pLysS cells.

Overexpression and purification of wtTIM and mutants was carried out as described by Vázquez-Contreras et al. (*14*). All TIM preparations were found to be homogeneous as determined by SDS−PAGE and anion-exchange FPLC analysis. The protein concentration of TIM variants was determined from the absorbance at 280 nm, using the same value for the absorption coefficient ($A^{1\%}_{1cm} = 10.0$) (*15*).

Activity Assays. Enzyme activity in the direction of DGAP to DHAP was determined by a coupled assay with α-glycerophosphate dehydrogenase (α-GDH), following NADH oxidation by absorbance changes at 340 nm (*16*). Assays were routinely made at 25 °C in a 1.0 mL mixture containing buffer A [100 mM triethanolamine (TEA), 10 mM EDTA, pH 7.4], 0.20 mM NADH, 0.019 mg of α-GDH, and 2.0 mM DGAP. The reaction was initiated by the addition of TIM (3.0 ng for wtTIM and C126A and 15 ng for C126S). For the determination of K_M^- and k_{cat}^-, the concentration of DGAP was varied between 0.05 and 4.0 mM. The kinetic parameters for the reverse reaction (K_M^+ and k_{cat}^+) were also determined by a coupled assay at 25 °C, using 0.20−10.0 mM DHAP as substrate in a 0.7 mL reaction mixture containing buffer A, 1.0 mM NAD, 4.0 mM arsenate, 0.120 mM dithiothreitol, and 1 unit of glyceraldehyde-3-phosphate dehydrogenase (*17*). The reaction was started with the addition of TIM (25 ng for wtTIM and 50 ng for C126S).

Fluorescence Spectroscopy and Fluorometric Titrations. Fluorescence measurements were made at 25 °C in a PC1 spectrofluorometer from ISS (Champaign, IL) equipped with a water-jacketed cell holder for temperature control. All experiments were done in buffer B (50 mM TEA, 5 mM EDTA, pH 7.4) filtered prior to each experiment. For spectral recordings, TIM solutions were excited at 280 nm, and emission was collected from 300 to 400 nm. Titrations were done using 0.050 mg mL^{-1} TIM solutions in the cell with successive additions of small aliquots from a concentrated 2-phosphoglycolate (PGA) solution to reach final concentrations in the 0.008−1.5 mM range; the total added volume of inhibitor was always less than 5% of the final volume. After each PGA addition, fluorescence intensity at 320 nm was recorded each second during 3 min to obtain a mean value and corrected by subtracting the buffer signal; the excitation wavelength was 280 nm. By assuming that the fluorescence intensities of the emitting species (free TIM and the PGA−TIM complex) are additive and considering how their concentrations are related through the equilibrium dissociation constant (K_I) for a 1:1 complex, we derived the expression:

$$Y = \left(\frac{a}{2E_t}\right)\left[(E_t + x + K_I) - \sqrt{(E_t + x + K_I)^2 - 4xE_t}\right] \quad (1)$$

where x is the total concentration of inhibitor in the cell and E_t represents the concentration of binding sites, whereas a (the asymptotic value to which Y tends at high x values) and K_I are the fitting parameters. Y equals $1 - (F/F_t)$, where F is the overall fluorescence intensity after each addition of

the inhibitor and F_t is the fluorescence of free TIM at the corresponding concentration, respectively. Fluorescence intensity of free TIM solutions proved to be quite linear with enzyme concentration within the range used in the titration experiments. Equation 1 was fitted to the experimental data by a nonlinear least-squares regression, using the program Origin (MicroCal, Inc., Northampton, MA).

Isothermal Titration Calorimetry. ITC experiments were performed using the high-precision VP-ITC titration calorimeter (Microcal, Inc.). All experiments were done in buffer B. TIM solutions were diafiltrated extensively in a stirred cell through polyether sulfone ultrafiltration disks. The concentration of enzyme was determined spectrophotometrically after thorough degassing of the solutions by evacuation; final concentrations in the sample cell were between 0.022 and 0.095 mM monomers. The concentration of PGA in the syringe was 1.5 or 3.0 mM. The titration schedule consisted of 25−28 consecutive injections of 3.0−8.0 μL with a 4 min interval between injections. To determine the heats of dilution of the ligand, titrations were performed under identical conditions but with buffer alone in the sample cell. These values were subtracted from the measured heats of binding. The binding constant (K_b), the enthalpy change (ΔH_b), and the stoichiometry (n) were determined by nonlinear fitting of normalized titration data using the expression corresponding to identical and independent binding sites (*18*).

Circular Dichroism Spectroscopy. Solutions of wtTIM and of its Cys126 mutants were equilibrated against 10 mM sodium phosphate buffer, pH 7.4, containing 1.0 mM EDTA. Their CD spectra were obtained at 20 °C in the far-UV region with a JASCO J-715 spectropolarimeter (Jasco Inc., Easton, MD) equipped with a PTC-348WI Peltier-type cell holder for temperature control; enzyme solutions of 0.10 mg mL^{-1} were used in a 0.10 cm cell. Each spectrum was the average of three repetitive scans and was corrected by the buffer signal. Ellipticities are reported as mean residue ellipticity [θ]. Thermal denaturation transitions were followed by continuously monitoring ellipticity changes at 220 nm, while the sample temperature was increased at 2.0 °C min^{-1}. Typically, TIM solutions of 0.010 mg mL^{-1} in a 1.00 cm cell with continuous stirring were used. Actual temperatures within the cell were registered with the external probe of the cell holder. Renaturation profiles were recorded after the denaturation transition had been completed; cooling was also controlled through the Peltier accessory.

Unfolding and Refolding Kinetics. The unfolding kinetics of the C126A and C126S TIM mutants were followed by changes in ellipticity at 220 nm, as reported by Benítez-Cardoza et al. (*19*). Briefly, a small aliquot of concentrated TIM solution was injected into a 1.00 cm cell containing buffer (50 mM Tris, pH 8.5) previously equilibrated at the working temperature and submitted to continuous stirring. Some experiments were done at pH 7.4 in 20 mM Tris buffer. Kinetic data were adjusted to a single exponential decay equation, $\theta_t = \theta_f + (\theta_0 - \theta_f) \exp(-k_u t)$, where θ_t is the ellipticity measured at time t, θ_f is the final ellipticity value, θ_0 represents the corresponding value at zero time, and k_u is the unfolding rate constant. The refolding kinetics of mutants was monitored by means of CD at 220 nm according to Benítez-Cardoza et al. (*19*). TIM was first denatured at 51 °C (C126S) or at 56 °C (C126A) during 90 s, time sufficient to attain more than 95% of unfolding. Then, the temperature in the Peltier cell holder was set to a value 3.0 °C below the desired refolding temperature; this allowed fast cooling (approximately 15 °C min^{-1}) of the enzyme solution. When the temperature in the cell was 0.5 °C above the desired value, the setting was raised to its final value. Kinetic data were adjusted to a second-order reaction equation, $\theta_t = \theta_f + (\theta_0 - \theta_f)/(2C_0k_rt + 1)$, where C_0 is the total molar concentration of TIM monomers, k_r is the refolding rate constant, and the other parameters were already described above. Monomer concentration was varied between 0.56 and 1.9 μM. Most studies were carried out at pH 8.5 in 50 mM Tris; in experiments accomplished at pH 7.4, 20 mM Tris buffer was used.

RESULTS

Expression and Structural Properties of Mutants. *E. coli* cultures containing the plasmid for the expression of the TIM mutants (C126S and C126A) grew slower than the culture containing wtTIM. Furthermore, the yields of both mutant isomerases were lower than that observed for wtTIM: 3.0 and 1.0 mg/L of culture for C126S and C126A, respectively, compared to 13.0 mg/L of culture for wtTIM. Denaturing gels of whole cell extracts revealed that lower yields for the mutant enzymes can be explained by lower expression levels. On the other hand, the secondary and tertiary structures of the mutant enzymes were not significantly different from those of wtTIM as judged by their far-UV CD and fluorescence spectra (Figure 1). The near-UV CD spectrum of the C126S enzyme was nearly superimposable on that of wtTIM (data not shown).

Catalytic Properties. When DGAP was used as substrate, kinetic data showed that k_{cat} and K_M for mutants C126A and C126S decrease in relation to wtTIM (Table 1). However, such decrements are not impressive at all and occur in a compensating way, so that k_{cat}/K_M is practically insensitive to any of these mutations. Experiments performed at 37 °C with the same substrate (results not shown) indicated only minute changes in k_{cat}/K_M values for each of the three enzymes comparatively to its values at 25 °C. Kinetic parameters with DHAP as substrate (Table 1) were also determined for wtTIM and the C126S mutant. As can be seen in Table 1, the cysteine to serine substitution resulted in small, compensating decreases in k_{cat} and K_M, paralleling the effect observed with DGAP as substrate. Clearly, the mutant retains a large catalytic efficiency, which is about 50% of that for wtTIM.

Phosphoglycolate-Binding Parameters. The binding of PGA by *S. cerevisiae* TIM and its mutants was studied at 25 °C by means of fluorometry and isothermal calorimetry. An example of results obtained is presented in Figure 2, which shows the binding isotherms for the C126S enzyme determined by fluorometry (Figure 2A) and calorimetry (Figure 2B). Overall results are also summarized in Table 1. It can be noted that the calorimetric method systematically gave 2−4-fold larger values for the inhibitor−enzyme binding constant, K_b. This effect, which may be caused by the higher protein and PGA concentrations used in calorimetric experiments, could be a reflection of the nonideality of the binding interaction. Regardless of the method used, however, K_b displays a sequential increase, from wtTIM to the C126S mutant, that approximately correlates with the

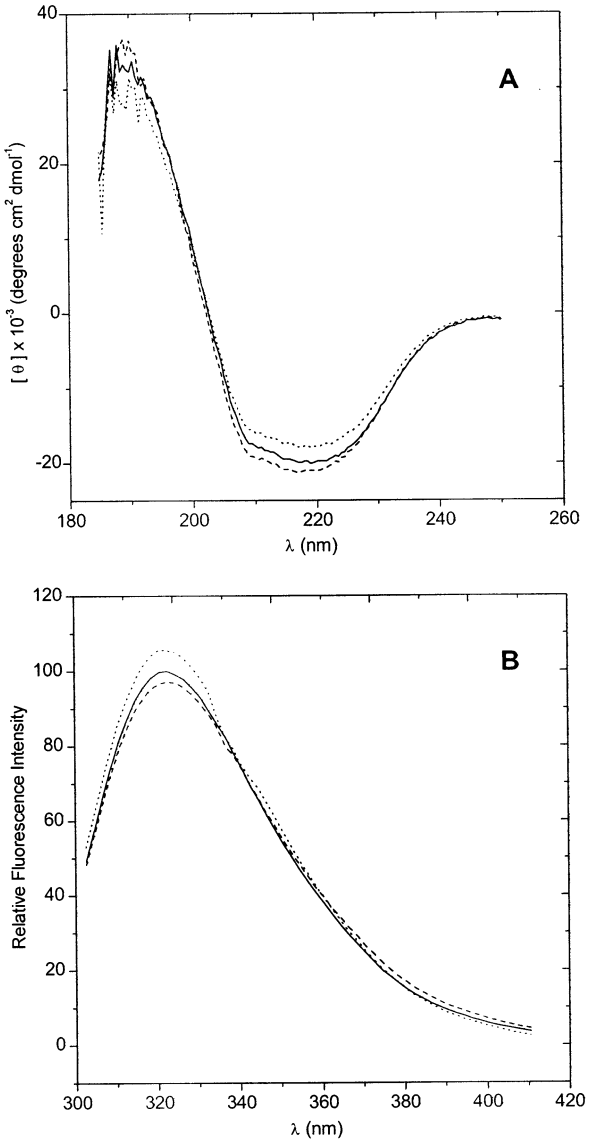

FIGURE 1: Spectroscopic properties of wtTIM and its Cys126 mutants. (A) Far-UV CD and (B) fluorescence spectra of wtTIM (solid lines), C126S (dashed lines), and C126A (dotted lines). CD spectra were recorded at 20 °C in 10 mM sodium phosphate and 1.0 mM EDTA, pH 7.4. TIM solutions of 0.10 mg mL^{-1} in a 0.100 cm cell were used. Fluorescence spectra were obtained at 25 °C using 0.050 mg mL^{-1} TIM solutions in 50 mM TEA and 5.0 mM EDTA, pH 7.4.

decrease in K_M and k_{cat}. Determinations of the thermodynamic binding functions showed that the reaction is enthalpically driven for all the three enzymes; however, the entropic contribution becomes less unfavorable for the association of PGA with the mutant enzymes.

Thermal Denaturation and Renaturation by Temperature Scans. Changes in secondary structure were continuously monitored by the ellipticity of protein solutions (0.010−0.015 mg mL^{-1}) at 220 nm, using a temperature ramp of 2.0 °C min^{-1}. As can be observed in Figure 3, unfolding−refolding curves for all the TIM forms display the hysteresis reported in previous studies of *S. cerevisiae* TIM (*19*); it is evident, however, that the recovery of secondary structure after one heating and cooling cycle is far from being complete for the Cys126 mutants (only about 65% of the native structure is recovered, as judged by CD spectra recorded after cooling).

Table 1: Kinetic and PGA-Binding Parameters for TIM and Its Cys126 Mutants[a]

	wtTIM	C126A	C126S
kinetic parameters			
k_{cat}^- (s^{-1})[b]	4.7 (0.7) × 10^3	3.1 (0.2) × 10^3	1.1 (0.2) × 10^3
K_M^- (mM)	1.1 (0.4)	0.8 (0.3)	0.3 (0.1)
k_{cat}^-/K_M^- (s^{-1} M^{-1})	4.3 × 10^6	3.9 × 10^6	3.7 × 10^6
k_{cat}^+ (s^{-1})[c]	0.5 (0.01) × 10^3	nd[f]	0.06 (0.01) × 10^3
K_M^+ (mM)	2.1 (0.16)	nd[f]	0.6 (0.03)
k_{cat}^+/K_M^+ (s^{-1} M^{-1})	2.2 × 10^5		1.0 × 10^5
binding parameters			
K_b (M^{-1})[d]	2.6 (0.5) × 10^4	3.6 (0.6) × 10^4	5.2 (1.1) × 10^4
K_b (M^{-1})[e]	4.1 (0.4) × 10^4	1.1 (0.5) × 10^5	1.2 (0.2) × 10^5
$\Delta G_b°$ (kcal mol^{-1})	−6.3 (0.3)	−6.9 (0.3)	−6.9 (0.1)
$\Delta H_b°$ (kcal mol^{-1})	−8.2 (0.8)	−8.5 (0.5)	−8.1 (0.5)
$T\Delta S_b°$ (kcal mol^{-1})	−1.9 (0.8)	−1.6 (0.5)	−1.2 (0.1)

[a] Kinetic parameters were determined in 100 mM TEA buffer and 10 mM EDTA, pH 7.4 at 25 °C. Substrate concentrations, DGAP and DHAP, were varied between 0.05 and 4.0 mM and between 0.02 and 10 mM, respectively. The binding constants of TIM variants to PGA were determined by fluorometric titration and isothermal titration calorimetry at 25 °C in 50 mM TEA buffer with 5 mM EDTA, at pH 7.4. Standard deviations are given in parentheses. [b] A (−) as superscript indicates D-glyceraldehyde 3-phosphate as substrate. [c] A (+) as superscript indicates dihydroxyacetone phosphate as substrate. [d] Fluorometrically determined. [e] Calorimetrically determined. [f] Not determined.

Similarly, the catalytic activity regained after cooling was approximately 70% of that shown by the unheated mutants.

On the high-temperature side of Figure 3 it is seen that unfolding transitions for both mutants are displaced to lower temperature compared to wtTIM. This decrease in the apparent T_m indicates that mutation of Cys126 induces some degree of destabilization in the TIM molecule, especially when cysteine is replaced by serine, in which case T_m is reduced by 13 °C. For the two mutants, changing pH from 8.5 to 7.4 resulted in a small 1.8 °C increment in T_m (results not shown). For wtTIM we had likewise found (*19*) that within the 7.2−9.1 pH range T_m was only slightly affected.

Because thermal unfolding−refolding transitions are far from an equilibrium situation, traditional data analysis cannot be applied to quantify the destabilizing effect of mutation. Thus, we determined the kinetic constants for unfolding and refolding of both mutants. As shown below, comparison of kinetic data presented in this work with those reported before (*19*) for wtTIM allowed for an estimation of the relative stability of the TIM variants under consideration.

Unfolding Kinetics of TIM Mutants. As observed before for yeast TIM, unfolding of its Cys126 mutants, when followed by far-UV CD, conformed well to simple first-order kinetics. Results obtained for the C126S enzyme are exemplified by the traces of $[\theta]_{220}$ shown in Figure 4; it is seen that unfolding proceeds to completion despite the temperature at which the experiment was conducted. It is worth mentioning that CD spectra recorded after unfolding of the mutated proteins (not shown) were very similar to that reported for thermally unfolded wtTIM (*19*). As has been discussed previously (*19*), completeness of the unfolding reaction would be expected under conditions that further engagement of the unfolded state in subsequent reactions that, though being silent about far-UV CD, lead to the formation of

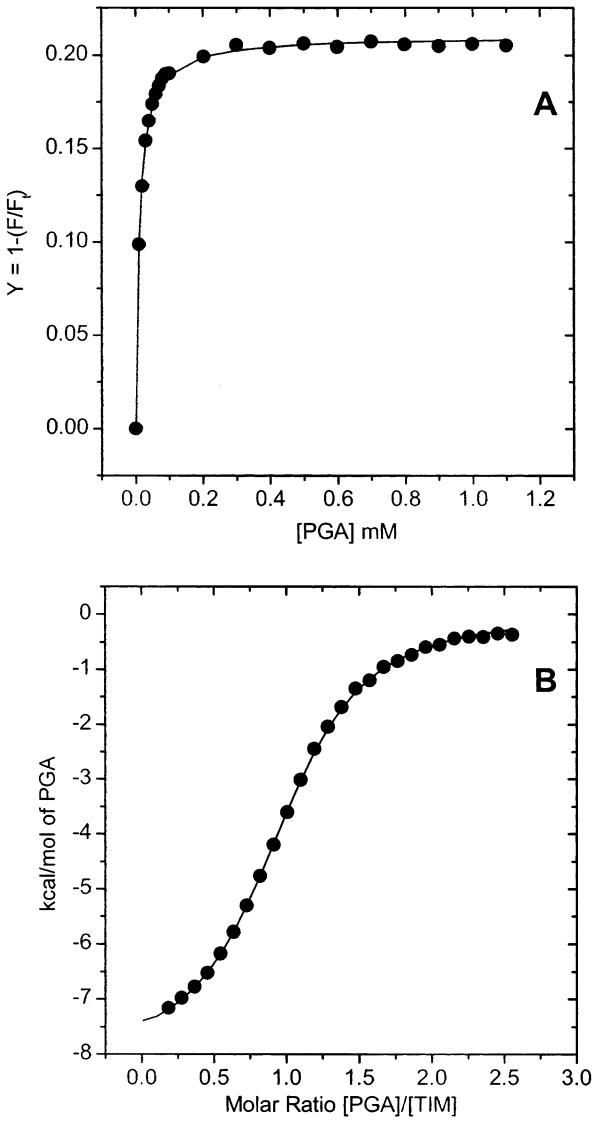

FIGURE 2: Binding isotherms of C126S TIM titrated with PGA. (A) Fluorometric titration of 1.85 μM C126S with 20 different additions of the inhibitor. Symbols represent the fraction of total TIM fluorescence (F_t) that is quenched by the added PGA; data points were fitted to eq 1 (see text) by a nonlinear regression (solid line). (B) Calorimetric titration of 95 μM C126S with 26 consecutive injections of 8.0 μL of 1.5 mM PGA. Symbols stand for the measured heats evolved during each inhibitor addition, normalized by the quantity of added PGA. The solid line represents the best fitting curve calculated from an identical and independent binding sites model. Both titrations were done at 25 °C in 50 mM TEA and 5 mM EDTA, pH 7.4.

irreversibly denatured species. Nevertheless, at temperatures where unfolding is fast, rapid cooling of the unfolded mutants to low temperatures permitted reasonable recoveries of structure and enzymatic activity (see below). The degree of reversibility attained upon refolding decreased with the time the unfolded proteins had been left standing at high temperature.

Values of the unfolding rate constant, k_u, determined at various temperatures are plotted in Figure 5A according to Eyring's equation:

$$\ln(k_u/T) = \ln E + \Delta S^{N\rightarrow TS}/R - (\Delta H^{N\rightarrow TS}/R)(1/T) \quad (2)$$

where E represents a preexponential factor; $\Delta H^{N\rightarrow TS}$ and

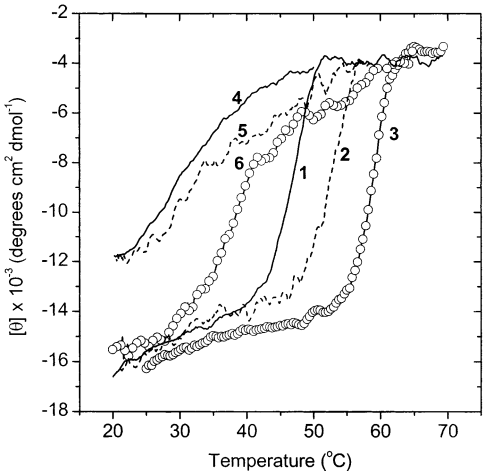

FIGURE 3: Thermal unfolding and refolding transitions of wtTIM and its Cys126 mutants. All thermal transitions were obtained at a heating or cooling rate of 2.0 °C min^{-1} at pH 8.5 in 50 mM Tris buffer: curves 1 and 4, C126S; curves 2 and 5, C126A; curves 3 and 6, wtTIM. Transitions were monitored by recording the ellipticity at 220 nm. Enzyme solutions of 0.010 mg mL^{-1} in a 1.00 cm cell with continuous stirring were used. Renaturation profiles were recorded immediately after denaturation transition had been completed.

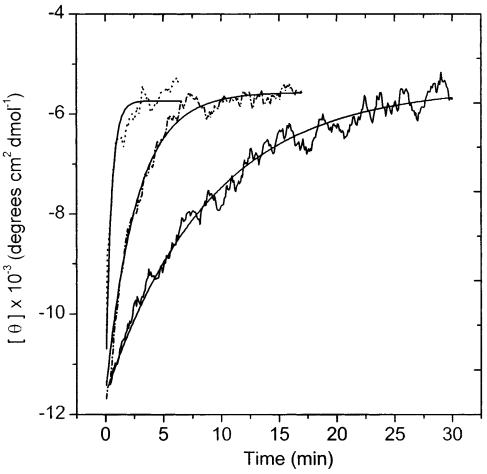

FIGURE 4: Time course of C126S thermal unfolding at different temperatures. Data shown correspond to the following temperatures: 43.8 °C (solid line), 47.3 °C (dash−dotted line), and 51.9 °C (dotted line). Ellipticity changes of 0.010 mg mL^{-1} enzyme solutions at pH 8.5 in 50 mM Tris were followed at 220 nm and fitted to a single exponential decay equation (smooth lines).

$\Delta S^{N\rightarrow TS}$ stand for the enthalpy and entropy changes, respectively, occurring during formation of the main transition state (TS). For comparison, the plot corresponding to wtTIM (*19*) is also shown in Figure 5A. It is immediately apparent the higher kinetic instability of the native C126S enzyme, especially at low temperature. Linear fits to data points in Figure 5A showed, in addition, that the cysteine to serine change causes a large reduction in $\Delta H^{N\rightarrow TS}$ (Table 2). The effect of this mutation was also studied at pH 7.4 (Table 2). $\Delta H^{N\rightarrow TS}$ was observed to increase slightly (by 7 kcal mol^{-1}), whereas the value of k_u extrapolated to 36.5 °C was only 1.6-fold reduced with respect to its value at pH 8.5.

Refolding Kinetics of the Mutants. To follow the regain of secondary structure upon renaturation, samples of the mutants were rapidly unfolded at high temperature and then quickly cooled as described in Materials and Methods. Figure

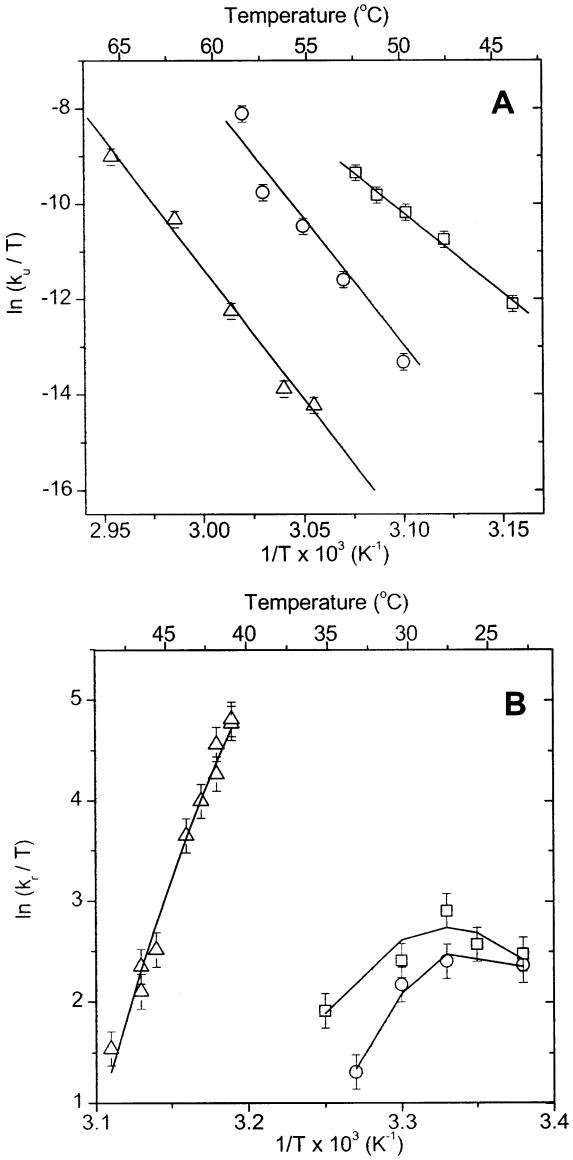

FIGURE 5: Eyring's plots for the rate constants of unfolding (k_u) and refolding (k_r) of wtTIM and its Cys126 mutants. (A) Denaturation and (B) renaturation rate constants were determined at pH 8.5 from far-UV CD. Data shown correspond to wtTIM (△), C126S (□), and C126A (○). For wtTIM, data are taken from ref *19*. Lines correspond to least-squares regressions according to equations described in the text (Materials and Methods section).

6 shows the time course of $[\theta]_{220}$ during refolding of the C126S enzyme at 30 °C and two different protein concentrations. It is evident from these curves the dependence of the refolding half-life with concentration. Furthermore, the plot in the inset to Figure 6 shows that the concentration dependence of $t_{1/2}$ is consistent with that expected for a second-order reaction [i.e., $t_{1/2} = 1/(2k_rC_0)$] with a rate constant (k_r) of $(3.3 \pm 0.3) \times 10^3$ M^{-1} s^{-1}. This value is in good agreement with the average k_r [$(3.7 \pm 0.4) \times 10^3$ M^{-1} s^{-1}] determined by fitting individual curves to second-order kinetics.

Refolding studies of both TIM mutants were performed in the 23−36.5 °C range, using protein solutions of 0.020−0.040 mg mL^{-1}. Independently of protein concentration and temperature of the experiment, the percentage of refolding was approximately 60−65%, as indicated by the final $[\theta]_{220}$ values, whereas enzymatic activity (measured at 25 °C) was

Table 2: Unfolding−Refolding Kinetics and Thermodynamics for wtTIM and Its Cys126 Mutants[a]

pH 8.5	wtTIM[b]	C126S	C126A
$\Delta H^{N\rightarrow TS}$ (kcal mol^{-1})	114 (2)	68 (3)	101 (10)
k_u, 27 °C (s^{-1})	2.1 (0.9) × 10^{-11}	4.6 (1.3) × 10^{-6}	5.0 (3.0) × 10^{-9}
$\Delta H^{2U\rightarrow TS}$, 27 °C (kcal mol^{-1})	43 (10)	0	0
k_r, 27 °C (s^{-1} M^{-1})	5.0 (4.5) × 10^4	5.3 (0.8) × 10^3	3.3 (0.4) × 10^3
$\Delta G^{2U\rightarrow N}$, 27 °C (kcal mol^{-1})	−21.1 (0.6)	−12.5 (0.2)	−16.2 (0.4)
$\Delta C_p^{2U\rightarrow N}$ (kcal mol^{-1} K^{-1})	−7.4 (1.7)	−6.0 (1.2)	−6.9 (1.2)
$\Delta H^{2U\rightarrow N}$, 27 °C (kcal mol^{-1})	−71 (10)	−68 (3)	−101 (10)
$T\Delta S^{2U\rightarrow N}$, 27 °C (kcal mol^{-1})	−50	−56	−85

pH 7.4	wtTIM	C126S
$\Delta H^{N\rightarrow TS}$ (kcal mol^{-1})	132 (5)	75 (2)
k_u, 36.5 °C (s^{-1})	7.2 (3.8) × 10^{-9}	9.3 (2.0) × 10^{-5}
k_r, 36.5 °C (s^{-1} M^{-1})	8.0 (4.0) × 10^4	2.3 (0.3) × 10^3
$\Delta G^{2U\rightarrow N}$, 36.5 °C (kcal mol^{-1})	−18.5 (0.5)	−10.5 (0.2)

[a] Rate constants were determined from far-UV CD measurements at different temperatures. Values shown were obtained either by direct determinations at or from extrapolation to the temperature indicated. Thermodynamic functions for refolding were calculated by assuming a two-state model. Standard deviations are given in parentheses. [b] Data for wtTIM, at pH 8.5, from results reported in ref *19*.

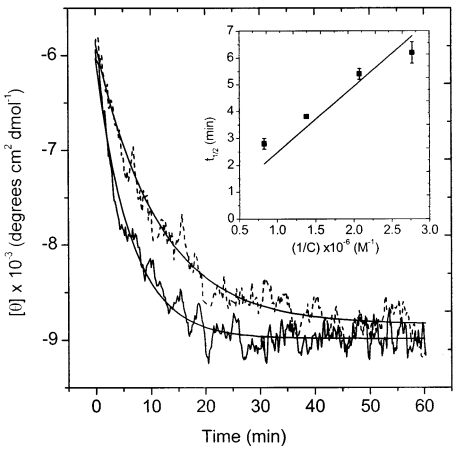

FIGURE 6: Refolding kinetics of C126S at 30 °C and two different enzyme concentrations. Data shown correspond to 0.030 mg mL^{-1} (dashed line) and 0.050 mg mL^{-1} (solid line), both in 50 mM Tris, pH 8.5. Kinetics were followed by changes in ellipticity at 220 nm. Data points were adjusted to a second-order reaction equation (smooth lines). The inset shows the effect of protein concentration on the half-life of C126S refolding. Concentration is expressed in terms of monomers.

recovered to 60−70%. That the degree of reversibility is nearly constant under the range of conditions mentioned above suggests that formation of irreversibly denatured species is not important during refolding itself but rather takes place at the higher, unfolding temperatures. Therefore, in calculating refolding rate constants we assumed that only 65% of the unfolded protein was competent for refolding, which introduced a small correction in the values of k_r. The temperature dependence of k_r is shown in Figure 5B. Eyring's plots for the two mutants display the downward curvature

typical of refolding or coupled refolding−association phenomena (ref *19* and references cited therein). Data fit to Eyring's equation with a finite heat capacity of activation, $\Delta C_p^{2U\rightarrow TS}$, was done according to the expression (*19*):

$$\ln(k_r/T) = A - B(1/T) - (\Delta C_p^{2U\rightarrow TS}/R)\ln(1/T) \quad (3)$$

where the value of B, $B = (\Delta H - \Delta C_p^{2U\rightarrow TS} T_r)/R$, enables one to compute the activation enthalpy at any given temperature, T_r. For C126A $\Delta C_p^{2U\rightarrow TS}$ was evaluated as -6.9 ± 1.2 kcal mol^{-1} K^{-1}, in rough agreement with the value for wtTIM (-7.4 ± 1.7 kcal mol^{-1} K^{-1}), whereas for C126S the heat capacity of activation was somewhat smaller (-6.0 ± 1.2 kcal mol^{-1} K^{-1}). Maximal values of k_r, which are reached at approximately 27 °C, are listed in Table 2; this table also shows k_r values for wtTIM and C126S determined near physiological conditions (pH 7.4, 36.5 °C).

DISCUSSION

It is currently accepted that an important contribution to the catalytic efficiency of TIM could come from modulating the polarity of the catalytic Glu165 environment. Residues located near this glutamate, such as Ser96 and Cys126, would then be expected to play a relevant role in this respect. According to our results, substituting Cys126 by Ser, a much less hydrophobic side chain, causes about 4-fold drops in both k_{cat} and K_M (Table 1). In contrast, smaller drops are observed when Cys is changed to Ala, a residue of similar hydrophobicity but significantly smaller in size. Either of these mutations, however, causes only a minor decrease in the k_{cat}/K_M value compared to wtTIM; indeed, the observed alterations of k_{cat}/K_M are even smaller than the variation found among TIMs from different organisms. It is worth recalling that, because the intracellular concentrations of DHAP and DGAP are generally below the K_M value [i.e., in yeast the reported concentrations are 0.3 and 0.4−1.2 mM, respectively (*20*)], the enzyme probably functions far from saturation in vivo conditions, and thus k_{cat}/K_M would be the determinant parameter for its activity. On these accounts, Cys126 could hardly be regarded as essential for the isomerase activity; that is, mutations C126A and C126S are probably neutral from the point of view of enzyme catalysis.

Because the rate of the reaction catalyzed by TIM is thought to be limited by diffusion of DHAP and DGAP into, and out of, the active site, a mutation that causes the enzyme to bind more tightly its substrate, product, or another reaction intermediate may lead to drops not only in K_M but also in k_{cat}; this is possibly happening with mutants C126A and C126S, whose affinities for PGA are increased relative to wtTIM. As shown in Table 1, the stronger binding of PGA to the mutants is mainly due to a less unfavorable entropy change. Because TIM−PGA binding involves several charge−charge interactions between active site residues and the inhibitor, it is appealing to interpret the less unfavorable ΔS_b as resulting from more extensive desolvation during binding.

Stability. The presence of hysteresis in protein unfolding−refolding transitions has been documented in an increasing number of reports. Most probably, this phenomenon has its origin in the slow kinetics of unfolding or refolding under certain conditions (*19*, *21*), which hinders achieving of equilibrium among the participating molecular states; further complications arise because of the tendency of unfolded states to aggregate. Thus the decrease in T_m observed for TIM mutants (Figure 3) should be taken as an indication of diminished kinetic, rather than thermodynamic, stability of the native dimer. Nevertheless, kinetic and calorimetric studies of the thermally induced unfolding and refolding of wtTIM (*19*) suggest that a simple two-state model is a good descriptor of the operating equilibrium: $N \rightleftarrows 2U$. In this model, the refolding reaction leads to formation of the native secondary structure. Though subsequent rearrangements of tertiary structure may be needed for recovery of enzymatic activity, the two-state model seemingly accounts for the overall stability of dimeric TIM. Results presented in this work show that the essentials of the two-state model are likely to be conserved for the conformational equilibrium in C126S. For the sake of a comparative evaluation of stability, we assumed that the same model also applies to the other mutant. Standard free energies for refolding were then calculated from

$$\Delta G^{2U\rightarrow N} = -RT\ln K_r \quad (4)$$

where K_r is given by the quotient k_r/k_u. Values of $\Delta G^{2U\rightarrow N}$ for the three TIM variants (27 °C, pH 8.5) are listed in Table 2; the corresponding enthalpies and entropies for refolding are also indicated. As can be seen from Table 2, stability notably decreases in the order wtTIM, C126A, C126S. Relative destabilization values, expressed as $\Delta\Delta G = \Delta G_{mutant} - \Delta G_{wt}$, are 4.9 and 8.6 kcal mol^{-1} for the Ala and Ser substitutions, respectively. The former value is in good agreement with the apparent $\Delta\Delta G$ of 5.4 kcal mol^{-1} found by Silverman and Harbury (*11*) for the same mutation. The magnitudes of $\Delta\Delta G$ are too large to be accounted for only by the different hydrophobicities of the side chains involved in mutation: on the basis of transfer free energies (*22*), the replacement of a buried Cys residue for Ala and Ser would be expected to destabilize the native state by at most 1.2 and 1.6 kcal mol^{-1}, respectively. As mentioned by various authors (*23*−*25*), when the substitution of a buried hydrophobic residue for another of smaller size leaves a cavity in the native structure, the destabilizing effect is larger (about 1.8 and up to 2.5 kcal mol^{-1} per methylene group deleted). Hence, if Cys is regarded as a typical hydrophobic side chain, and accounting for its size, the maximum destabilization expected for a Cys to Ala mutation would be between 3.0 and 4.0 kcal mol^{-1}, in reasonable agreement with the experimental $\Delta\Delta G$ value. On the other hand, the much larger $\Delta\Delta G$ for the C126S mutant points out the occurrence of more drastic alterations in the forces determining TIM stability; for instance, an increase in solvent accessibility in the native molecule could be occurring after mutation (*23*).

Further insight into the causes of destabilization can be sought in comparisons of thermodynamic properties other than free energy. From data in Table 2 it is readily seen that there is no correlation between ΔG and ΔH values (or the corresponding entropic terms) for the refolding of TIM variants; similar lack of correlation has been observed with other proteins (*26*). What is important, however, is to determine whether relative changes in thermodynamic functions can be correlated with alterations in the molecular properties thought to be determining for protein stability. To this end we applied here the simple model in which thermodynamic functions are parametrized in terms of the

polar and apolar surface areas that become buried upon folding (*27*). According to this approach, $\Delta H^{2U\rightarrow N}$ and $\Delta C_p{}^{2U\rightarrow N}$ can be expressed as

$$\Delta H^{2U\rightarrow N} = \Delta H^{*}\Delta \mathrm{ASA}_{pol} + \Delta C_p{}^{2U\rightarrow N}(T - T_H{}^{*}) \quad (5)$$

$$\Delta C_p{}^{2U\rightarrow N} = \Delta C_{p,pol}\Delta \mathrm{ASA}_{pol} + \Delta C_{p,ap}\Delta \mathrm{ASA}_{ap} \quad (6)$$

where $\Delta \mathrm{ASA}_{pol}$ and $\Delta \mathrm{ASA}_{ap}$ represent changes in solvent-accessible polar and apolar surface area upon refolding; parameters appearing in these equations [$\Delta H^{*} = 35$ cal (mol Å^2)$^{-1}$; $\Delta C_{p,pol} = -0.26$ cal K^{-1} (mol Å^2)$^{-1}$; $\Delta C_{p,ap} = 0.45$ cal K^{-1} (mol Å^2)$^{-1}$; $T_H{}^{*} = 373$ K (100 °C)] have been derived from studies of a number of proteins and model compounds (*27*). Description of the refolding thermodynamics is completed by writing the entropic term:

$$T\Delta S^{2U\rightarrow N} = T\Delta S^{conf} + T\Delta C_p{}^{2U\rightarrow N}\ln(T/T_s{}^{*}) \quad (7)$$

where $T_s{}^{*}$ is 385 K (112 °C); ΔS^{conf} stands for the entropic contribution from conformational changes during the process and is assumed to be proportional to the number of residues in the molecule. By solving eqs 5 and 6 with data for wtTIM, it is found that 17500 Å^2 of polar area and 26600 Å^2 of apolar area are buried upon refolding. The average total buried area per amino acid residue would be close to 90 Å^2, slightly less than the 95−100 Å^2 per residue determined for proteins larger than 200 residues (*27*). From eq 7, ΔS^{conf}, when normalized as a per residue basis, equals −4.1 cal K^{-1} (mol of residue)$^{-1}$, again a little smaller than the −4.3 cal K^{-1} (mol of residue)$^{-1}$ determined from several proteins (*27*). These results may be indicative of some residual structure persisting in thermally unfolded TIM, as suggested in our previous work (*19*). In any case, the empirical parametrization seems to describe well the unfolding−refolding of wtTIM, at least to permit comparisons among its variants. Computations with data of C126A indicated the same $\Delta \mathrm{ASA}_{pol}$ and ΔS^{conf} as in wtTIM, whereas $\Delta \mathrm{ASA}_{ap}$ was about 1000 Å^2 less for the mutant. Though these results seem to be consistent with a decrease in stability due mainly to the formation of a hydrophobic cavity in the folded mutant, the value of $\Delta \mathrm{ASA}_{ap}$ is numerically doubtful because of the uncertainty in the calculated buried areas (approximately ±2500 Å^2). For the C126S mutant, in contrast, computations resulted in significantly large reductions in both $\Delta \mathrm{ASA}_{pol}$ (approximately 3000 Å^2) and $\Delta \mathrm{ASA}_{ap}$ (approximately 5000 Å^2), compared to wtTIM; ΔS^{conf} for this mutant was −3.4 cal K^{-1} (mol of residue)$^{-1}$. Such large reductions in buried areas and in ΔS^{conf} appear to be too large to be caused solely by substitution of an internal hydrophobic residue by a more polar one. More likely, they could reflect perturbations that extend beyond the vicinity of residue 126. A clue on how the buried area would be reduced by the mutation C126S can be found in an examination of recently determined high-resolution TIM structures (*5*, *28*). This analysis reveals that, regardless of the presence or absence of ligand in the active site, the atom S_γ of Cys126 occupies a key position where it might play a double role: First, it seemingly acts as a seal for the β-barrel core by making hydrogen bonds with the main-chain oxygens of Ile124 and Leu93, whose side chains are constituents of the barrel inner core. Second, the S_γ atom is located at van der Waals distance (approximately 4.1 Å) from the $O_\epsilon 2$ of the catalytic glutamate, thus forming part of the active site "bottom" wall. Although solvent molecules pervade the active site region, none of these directly interacts with the S_γ; its three nearest neighbor waters are located 5.0−6.0 Å away. One of these molecules forms a hydrogen bond with the $O_\epsilon 2$ of the catalytic glutamate, whereas the other two do the same with residues located in loops 3 (the monomer−monomer interdigitating loop), 4, and 7 or in β strands 4, 7, and 8. It is reasonable then that in C126S the hydrophilic character of the Ser side chain may affect the distribution of solvent molecules in a relatively large region of the protein, thereby leading to a native mutant more hydrated than wtTIM. Furthermore, this proposal would be consistent with a larger desolvation occurring when ligands bind to C126S, as discussed above for binding entropies.

Whatever the causes of the low stability observed for C126S, it is evident that this mutation could lessen the level of native TIM in vivo. For instance, taking the TIM concentration of 1.24 mg mL^{-1} found in *S. cerevisiae* (*20*) as a representative value and using data reported in Table 2, it is calculated that near physiological conditions about 2% of the mutated enzyme would be unfolded. In contrast, under similar conditions the estimated fraction of unfolded wtTIM would be about 1000 times smaller. The presence of significant amounts of unfolded or misfolded monomers can then lead to a depletion of native enzyme because of their tendency to form aggregates or other irreversibly denatured species. Moreover, unspecific aggregation may represent a serious drawback since a nascent polypeptide folds in a crowded cytoplasm. Therefore, mutations that reduce the folding rate, such as C126S and C126A, would be expected to slow the expression and decrease the yield of functional enzyme. Besides, both of these TIM mutants apparently showed greater propensity to suffer irreversible denaturation than wtTIM. Whether or not Cys126 plays some role in avoiding undesirable side reactions of unfolded or partially unfolded TIM is yet an open question.

In summary, our results point out that constraints on the evolutionary mutation of Cys126 are probably much more related to requirements for efficient folding and stability of native TIM than to maintaining its catalytic efficiency. In this regard, it should be mentioned that Ile124 has been identified as a component of a putative folding nucleus in the TIM family of proteins (*29*). Recalling that this Ile is hydrogen-bonded to the S_γ atom of Cys126 and that both of these residues occur in a conserved motif (IXCXG), it is likely that such a folding nucleus would comprise all residues in the motif. Similarly, a recent mutational study (*30*) on the role of the conserved R189-D225 salt bridge suggests that this ionic interaction, which links helices 6 and 7 to each other, forms part of another possible nucleation site (*29*). Additional studies on the mechanism of TIM refolding are clearly required to elucidate the participation of various conserved residues in achieving a fast-folding, stable native dimer. For Cys126 particularly, it remains to be explored what properties display other TIM variants resulting from single mutation at this position.

ACKNOWLEDGMENT

We thank Dr. Alejandro Fernández-Velasco (Facultad de Medicina, UNAM, México) for help with protein purification

by FPLC, Dr. Adela Rodríguez-Romero (Instituto de Química, UNAM, México) for advice on ITC determinations, Dr. Georgina Garza-Ramos (Facultad de Medicina, UNAM, México) for assistance in activity assays using DHAP, and M. C. Lorena Ruíz-Paniagua for help with construction of the mutants.

REFERENCES

1. Raines, R. T., Sutton, E. L., Straus, D. R., Gilbert, W., and Knowles, J. R. (1986) Reaction Energetics of a Mutant Triosephosphate Isomerase in Which the Active-Site Glutamate Has Been Changed to Aspartate, *Biochemistry 25*, 7142−7154.
2. Komives, E. A., Chang, L. C., Lolis, E., Tilton, R. F., Petsko, G. A., and Knowles, J. R. (1991) Electrophilic Catalysis in Triosephosphate Isomerase: The Role of Histidine-95, *Biochemistry 30*, 3011−3019.
3. Lodi, P. J., Chang, L. C., Knowles, J. R., and Komives, E. A. (1994) Triosephosphate Isomerase Requires a Positively Charged Active Site: The Role of Lysine-12, *Biochemistry 33*, 2809−2814.
4. Lolis, E., and Petsko, G. A. (1990) Crystallographic Analysis of the Complex between Triosphosphate Isomerase and 2-Phosphoglycolate at 2.5-Å Resolution: Implications for Catalysis, *Biochemistry 29*, 6619−6625.
5. Kursula, I., and Wierenga, R. K. (2003) Crystal Structure of Triosephosphate Isomerase Complexed with 2-Phosphoglycolate at 0.83-Å Resolution, *J. Biol. Chem. 278*, 9544−9551.
6. Sampson, N. S., and Knowles, J. R. (1992) Segmental Movement: Definition of the Requirement for Loop Closure in Catalysis by Triosephosphate Isomerase, *Biochemistry 31*, 8482−8487.
7. Lolis, E., Albert, T., Davenport, R. C., Rose, D., Hartman, F. C., and Petsko, G. A. (1990) Structure of Yeast Triosephosphate Isomerase at 1.9-Å Resolution, *Biochemistry 29*, 6609−6618.
8. Zhang, Z., Komives, E. A., Sugio, S., Blacklow, S. C., Narayana, N., Xuong, N. H., Stock, A. M., Petsko, G. A., and Ringe, D. (1999) The Role of Water in the Catalytic Efficiency of Triosephosphate Isomerase, *Biochemistry 38*, 4389−4397.
9. Blacklow, S. C., Liu, K. D., and Knowles, J. R. (1991) Stepwise Improvement in Catalytic Effectiveness: Independence and Interdependence in Combinations of Point Mutations of a Sluggish Triosephosphate Isomerase, *Biochemistry 30*, 8470−8476.
10. Zubillaga, R. A., Pérez-Montfort, R., and Gómez-Puyou, A. (1994) Differential Inactivation of Rabbit and Yeast Triosephosphate Isomerase: Effect of Oxidations Produced by Chloramine-T, *Arch. Biochem. Biophys. 313*, 328−336.
11. Silverman, J. A., and Harbury, P. B. (2002) The Equilibrium Unfolding Pathway of a $(\beta/\alpha)_8$ Barrel, *J. Mol. Biol. 324*, 1031−1040.
12. Silverman, J. A., Balakrishnan, R., and Harbury, P. B. (2001) Reverse Engineering the $(\beta/\alpha)_8$ Barrel Fold, *Proc. Natl. Acad. Sci. U.S.A. 98*, 3092−3097.
13. Sambrook, J., and Russell, D. W. (2001) *Molecular Cloning: A Laboratory Manual*, 3rd ed., Cold Spring Harbor Laboratory Press, New York.
14. Vázquez-Contreras, E., Zubillaga, R. A., Mendoza-Hernández, G., Costas, M., and Fernández-Velasco D. A. (2000) Equilibrium Unfolding of Yeast Triosephosphate Isomerase: A Monomeric Intermediate in Guanidine-HCl and Two-State Behavior in Urea, *Protein Pept. Lett. 7*, 57−64.
15. Norton, I. L., and Hartman, F. C. (1972) Haloacetol Phosphates. A Comparative Study of the Active Sites of Yeast and Muscle Triosephosphate Isomerase, *Biochemistry 11*, 4435−4441.
16. Rozacky, E. E., Sawyer, T. H., Barton, R. A., and Gracy, R. W. (1971) Studies of Human Triosephosphate Isomerase: Isolation and Properties of the Enzyme from Erytocytes, *Arch. Biochem. Biophys. 146*, 312−320.
17. Hernández-Alcántara, G., Garza-Ramos, G., Mendoza Hernández, G., Gómez-Puyou, A., and Pérez-Montfort, R. (2002) Catalysis and Stability of Triosephosphate Isomerase from *Trypanosoma brucei* with Different Residues at Position 14 of the Dimer Interace. Characterization of a Catalytically Competent Monomeric Enzyme, *Biochemistry 41*, 4230−4238.
18. Wiseman, T., Williston, S., Brandts, J. F., and Lin, L.-N. (1989) Rapid Measurement of Binding Constants and Heats of Binding Using a New Titration Calorimeter, *Anal. Biochem. 179*, 131−137.
19. Benítez-Cardoza, C. G., Rojo-Domínguez, A., and Hernández-Arana, A. (2001) Temperature-Induced Denaturation and Renaturation of Triosephosphate Isomerase from *Saccharomyces cerevisiae*: Evidence of Dimerization Coupled to Refolding of the Thermally Unfolded Protein, *Biochemistry 40*, 9049−9058.
20. Albe, K. R., Butler, M. H., and Wright, B. E. (1990) Cellular Concentrations of Enzymes and Their Substrates, *J. Theor. Biol. 143*, 163−195.
21. Nájera, H., Costas, M., Fernández-Velasco, D. A., (2003) Thermodynamic Characterization of Yeast Triosephosphate Isomerase Refolding: Insights into the Interplay between Function and Stability as Reasons for the Oligomeric Nature of the Enzyme, *Biochem. J. 370*, 785−792.
22. Creighton, T. E. (1993) *Proteins: Structure and Molecular Properties*, 2nd ed., pp 153−161, W. H. Freeman, New York.
23. Lee, B. (1993) Estimation of the Maximum Change in Stability of Globular Protein upon Mutation of a Hydrophobic Residue to Another of Smaller Size, *Protein Sci. 2*, 733−738.
24. Jackson, R. M., and Sternberg, M. J. E. (1994) Application of Scaled Particle to Model the Hydrophobic Effect: Implications for Molecular Association and Protein Stability, *Protein Eng. 7*, 371−383.
25. Fersht, A. (1999) *Structure and Mechanism in Protein Science: A guide to enzyme catalysis and protein folding*, pp 532−534, W. H. Freeman, New York.
26. Connelly, P., Ghosaini, L., Hu, C.-Q., Kitamura, S., Tanaka, A., and Sturtevant, J. M. (1991) A Differential Scanning Calorimetric Study of the Thermal Unfolding of Seven Mutant Forms of PhageT4 Lysozyme, *Biochemistry 30*, 1887−1871.
27. Murphy, K. P., and Freire, E. (1992) Thermodynamics of Structural Stability and Cooperative Folding Behavior in Proteins, *Adv. Protein Chem. 43*, 313−361.
28. Rodríguez-Romero, A., Hernández-Santoyo, A., del Pozo Yauner, L., Kornhauser, A., and Fernández-Velasco, D. A. (2002) Strucutre and Inactivation of Triosephosphate Isomerase from *Entamoeba histolytica*, *J. Mol. Biol. 322*, 669−675.
29. Kannan, N., Selvaraj, S., Gromiha, M. M., and Vishveshwara, S. (2001) Clusters in α/β Barrel Proteins: Implications for Protein Structure, Function, and Folding: A Graph Theoretical Approach, *Proteins 43*, 103−112.
30. Kursula, I., Partanen, S., Lambeir, A.-M., and Wierenga, R. K. (2002) The Importance of the Conserved Arg191-Asp227 Salt Bridge of Triosephosphate Isomerase for Folding, Stability, and Catalysis, *FEBS Lett. 518*, 39−42.

BI036077S